

Using Double Difference Information from Network Solutions to Generate Observations for a Virtual GPS Reference Receiver

A. Jäggi, G. Beutler, U. Hugentobler
Astronomical Institute,
University of Berne, Sidlerstrasse 5, CH-3012 Berne, Switzerland

Abstract. We develop the theoretical background for generating artificial observations for a virtual reference receiver in post processing mode. We use double difference information from network solutions to correct zero difference observations in a preprocessing clock estimation process and find that the observations can be adjusted on the level of about 4 mm. Using simple ionosphere and troposphere modeling techniques we show how phase observations can be calculated for any location within the network. Full use is made of the ambiguity and ionosphere information from double difference network solutions in order to keep full consistency of the artificial phase observations on the double difference level. The effect of such observations is demonstrated with data from a GPS network in Switzerland. We find that baseline solutions are more precisely determined (e.g. ambiguity resolution) using a virtual receiver at one end with observations constructed with the proposed approach.

Keywords. Virtual reference station, stochastic ionosphere, ambiguity resolution

1. Introduction

The still increasing number of continuously operated GPS arrays offers a wide range for testing and validating new positioning concepts. To make full use of the entire information in the case of phase, it is necessary for a user to perform a correct, double difference (dd) ambiguity-fixed network solution with all the data from the reference network and from the rover receiver. It makes sense to simplify the handling for the user by establishing artificial observations for one virtual reference receiver (VRR) out of the (real) observations from the reference receivers of the permanent array. The proposed procedure is based on the idea of using and removing a priori known information from network solutions of the reference sites and creating artificial zero difference (zd) observations for any location within the permanent array with a significantly smaller “observation” noise, reduced noise due to multi-



Fig. 1 AGNES stations in April 2001 (courtesy Swiss Federal Office of Topography).

path and an adequate modeled troposphere and ionosphere above the selected site. These observations can be used to perform a short baseline solution with any commercial software to the rover receiver which benefits (e.g. in ambiguity resolution) from the quality of artificial observations and from the short baseline length.

This paper first gives a short overview on the generation of virtual code observations. The main part consists of the development of phase observations for a VRR and the discussion of their benefits. We restrict ourselves to a post-processing procedure suitable to study the best-case scenario as well as for validating results from real time kinematic (RTK) applications. Each section closes with results with data from AGNES (Automated GPS Network in Switzerland), a multi-functional GPS permanent network which is operated by the Swiss Federal Office of Topography (L+T) and mainly serves for navigational and geodetic surveying purposes and scientific applications as well. Today the network consists of approximately 20 stations (Figure 1) with a typical spacing of 50 km (<http://swisstopo.ch/en/geo/agnes.htm>). All presented data stem either from the year 1999 when SA was on or from the year 2000 when SA was turned off. At that time the network only consisted of a pilot configuration of 6 resp. 10 stations.

2. Artificial Code Observations

Let us assume that we process all code data of all stations of a permanent GPS array in an epoch-by-epoch mode. In a first section we discuss the necessary preprocessing steps, in the following section the procedure to generate the artificial observations.

2.1 Preprocessing

For each epoch the code observation equation of the reference receivers $i = 1, \dots, n$ to the satellites $k = 1, \dots, s$ reads as

$$C_i^k = \rho_i^k - c \cdot \Delta t^k + c \cdot \Delta t_i + I_i^k + \Delta \rho_{i, trop}^k \quad (1)$$

with the observed pseudorange C_i^k , the geometric (slant) range ρ_i^k , the satellite and receiver clock corrections Δt^k and Δt_i , and the ionospheric and tropospheric refraction I_i^k and $\Delta \rho_{i, trop}^k$.

Provided precise satellite orbits are available (e.g. from IGS) as well as tropospheric zenith path delays from an ambiguity-free phase network solution (see Section 3.1) we may remove the terms ρ_i^k and $\Delta \rho_{i, trop}^k$ in Eq. (1). When analyzing the ionosphere-free linear combination (C_3) we are left with clock terms as the only unknowns:

$$c_i^k = -c \cdot \Delta t^k + c \cdot \Delta t_i \quad (2)$$

where c_i^k is the C_3 observable reduced by the a priori known information. By selecting either a satellite or a receiver clock as reference clock the system (2) can be solved for the unknown parameters (Bock *et al.*, 2000). Moreover this analysis provides post fit residuals which allow to clean the original data (outlier detection).

2.2 Artificial Observations

Removing the known geometry and atmospheric terms from Eq. (1) and adding the corresponding terms for the position \vec{r}_v of the VRR transforms the original observations to the new location and new atmospheric conditions:

$$\bar{C}_i^k = \rho_v^k - c \cdot \Delta t^k + c \cdot \Delta t_i + I_v^k + \Delta \rho_{v, trop}^k. \quad (3)$$

Note that by introducing Eq. (2), the new pseudo-observations \bar{C}_i^k contain already precise clock corrections. Considering the term for ionospheric path delay above the VRR in the case of code observations, it is sufficient to use I_v^k stemming from an ionosphere a priori model. Similar remarks are valid for the tropospheric path delay $\Delta \rho_{v, trop}^k$. Assuming that all reference receivers collected code observations to the same satellites we may define the artificial observations epoch-

wise by

$$\bar{C}_v^k := \frac{1}{n} \sum_{i=1}^n \bar{C}_i^k. \quad (4)$$

Such a definition leads to a observation noise $\sigma(\bar{C}) = \sigma(C)/\sqrt{n}$. If the assumption for Eq. (4) does not hold we may alternatively define as artificial observations:

$$\bar{C}_v^k := \frac{1}{n(k)} \sum_{i=1}^{n(k)} (\bar{C}_i^k - c \cdot \Delta t_i) \quad (5)$$

where $n(k)$ is the number of sites having actually observed satellite k . By this procedure the clock offset of the virtual receiver is set to zero with no implications on the later use of the observations.

It can be verified that coordinates of a VRR estimated by code point positioning (introducing precise satellite clocks) have a rms error which is smaller by approximately a factor \sqrt{n} compared to a real station at the same location (Jaeggi, 2001).

3. Artificial Phase Observations

For each epoch the phase observation equation for the reference receivers reads as

$$L_i^k = \rho_i^k - c \cdot \Delta t^k + c \cdot \Delta t_i - I_i^k + \Delta \rho_{i, trop}^k + \lambda \cdot N_i^k \quad (6)$$

with the observed phase pseudorange L_i^k and the initial ambiguity term $\lambda \cdot N_i^k$ where we used the same notation as in Eq. (1). The initial ambiguity term however changes the situation for generating artificial observations considerably. Applying Eq. (4) resp. Eq. (5) without any preparatory work to Eq. (6) would destroy the integer nature of the initial ambiguity terms. Therefore another approach described in the next section has to be selected.

3.1 Transformation of DD Ambiguities to Quasi ZD Ambiguities

Having performed an ambiguity free network solution for saving precise station coordinates and accurate troposphere zenith path delays, the dd carrier phase ambiguities N_{ij}^{kl} can be fixed to their integer values by performing a correct dd network solution (Mervart, 1995). For a network of the size of AGNES the Wide-lane, Narrow-lane approach is well suited (Beutler *et al.*, 1999). In the optimum case we have then access to all successfully resolved dd ambiguities on $n-1$ linearly independent baselines. Ambiguity resolution is mandatory for all further processing steps otherwise an observation has to be excluded. Based on these values we convert the terms N_{ij}^{kl} in the

network to a quasi zd level as follows:

$$N_i^k = N_{ref}^k + N_{i,ref}^k = N_{ref}^k + N_{i,ref}^{REF} + N_{i,ref}^{k,REF} \quad (7)$$

with a satellite specific zd term N_{ref}^k , a receiver specific single difference (sd) term $N_{i,ref}^{REF}$, and the known dd ambiguity term $N_{i,ref}^{k,REF}$. This conversion is described and validated by (Jaeggi, 2001). Due to a degree of freedom of $n + s - 1$ the method depends on two assumptions: (1) The choice of the values of $N_{i,ref}^{REF}$ on each baseline for a reference satellite, and (2) the choice of the values of N_{ref}^k for a particular reference station. We have to ensure that exactly the same dd ambiguities result when again forming double differences. Depending on the selected reference station this restriction may considerably reduce the number of well suited zd observations for generating artificial observations. Only files which are made perfectly coherent can be used without introducing any inconsistencies. The obtained zd ambiguities from Eq. (7) are biased by satellite specific terms (class I bias) and by receiver specific terms (class II bias). A class I bias is always the same at all stations for a given satellite and therefore cancels by forming single differences. A class II bias which can be caused by adjusting sd ambiguities on a quasi single difference level also cancels when again forming dd. It is important to note that finally artificial phase observations will be evaluated (see Section 3.4) again on dd level which implies that it is sufficient to prepare ambiguity information consistent on dd level.

3.2 Preprocessing

For each epoch we may define for the original carrier frequencies (L_1, L_2)

$$l_i^k := L_i^k - a_i^k - \lambda N_i^k \quad (8)$$

with the reduced phase pseudorange l_i^k , the observed phase pseudorange L_i^k , the a priori information a_i^k , and the quasi zd ambiguity term N_i^k , if a consistent term N_i^k is available. Provided precise satellite orbits are available (e.g. from IGS) and tropospheric zenith path delays (both included in term a_i^k) from an ambiguity-free phase network solution we are left with “clock” terms and “ionosphere” terms as the only unknowns:

$$l_i^k = -c \cdot \Delta t^k + c \cdot \Delta t_i - I_i^k. \quad (9)$$

The three terms on the right-hand side of Eq. (9) are all biased due to the biased term N_i^k in Eq. (8) and should therefore be called pseudo-clock and pseudo-ionosphere terms. By selecting one clock as reference clock the system (9) can be solved for the unknown parameters either by simultaneously processing Eq. (9) for

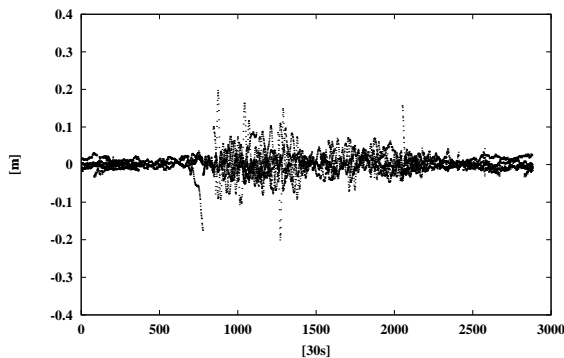


Fig. 2 Stochastic ionosphere parameters on a quasi single difference level over a 40.4 km baseline on day 299 in the year 2000. The fluctuation-level depends on the baseline length and the day-time.

L_1 and L_2 or by separately processing L_1 and L_2 by introducing appropriate ionosphere information (see Section 3.2.1). From the point of view of the parameter estimation process both methods are well suited, but the simultaneous processing of L_1 and L_2 has two disadvantages even if it would favour the error budget: (1) the estimated pseudo-ionosphere parameters are biased by class I and class II biases due to the term N_i^k and (2) all estimated parameters are influenced by L_1 and L_2 ambiguity terms. While the latter point only prevents a strict independency of the parameters on both frequencies the presence of class II biases in the former point makes an ionosphere interpolation impossible (see Section 3.3.1). Note that we have to avoid forming the ionosphere-free linear combination (L_3) in Eq. (9) in order not to destroy the preserved integer nature of the transformed ambiguity terms. Moreover L_3 amplifies random phase measurement noise and noise due to multipath.

3.2.1 Stochastic Ionosphere Parameters

Opposed to the deterministic component of the Total Electron Content (TEC) which is described by an ionosphere model the stochastic component of the TEC represents the residual part of the modeling which is due to a multitude of short-term fluctuations in the TEC. Using the fixed dd ambiguities these stochastic ionosphere parameters (SIP’s) can be computed on the dd level either by analyzing the $L_4 = L_1 - L_2$ linear combination or by simultaneously analyzing the original carriers L_1 and L_2 directly (Schaer, 1999). The main difference lies in an accuracy gain of approximately a factor of 4 when choosing the latter method. Figure 2 shows the stochastic component of the TEC in the AGNES network.

As we try to avoid forming any linear combination (L_4 contains only 64.7% of the ionospheric signal) we use the latter method for solving Eq. (9). In order to use the SIP’s in Eq. (9)

we convert them from dd to zd level. Again (as for the ambiguities, see Section 3.1) this conversion depends on two assumptions: (1) the choice of one $I_{i,ref}^{REF}$ for each baseline (or a summation condition on all SIP's on each baseline), and (2) the choice of the values of I_{ref}^k for a particular reference station. The second assumption causes a class I bias which is not critical but, more important, assumption (1) does not cause a class II bias stemming from the ambiguity term N_i^k which is essential and allows for a satellite-specific ionosphere interpolation (see Section 3.3.1). This step of the analysis provides quasi zd SIP's which can be applied in Eq. (9). It is important to note that these terms contain only the differential ionosphere which implies that a separate clock estimation for L_1 and L_2 gives pseudo clock parameters which are not only biased by the class I and class II biases caused by the ambiguity terms but also by ionospheric biases. Nevertheless this does not affect the parameter estimation at all. The remaining ionospheric effect can be absorbed by the clock parameters and shows up in the differences of $(\Delta t_{i,L_1} - \Delta t_{i,L_2})$ resp. $(\Delta t_{L_1}^k - \Delta t_{L_2}^k)$ (Jaeggi, 2001). Figure 3 shows all L_1 residuals from a clock estimation process (9) for one day in the AGNES network.

Applying SIP's and transformed ambiguities stemming from Eq. (7) leads to L_1 residuals in the order of 4 mm which are free from any remaining systematics. Only the processing of L_1 and L_2 simultaneously as described in the last section would lower the residuals slightly by an approximate factor of $\sqrt{2}$ quite close to the random phase measurement noise level. Figure 4 shows the impact of the different approaches discussed in this section on the resulting accuracy.

3.3 Artificial Observations

A transformation equivalent to Eq. (3) allows to define artificial carrier phase observations in full analogy to Eq. (4) resp. Eq. (5). Note that such

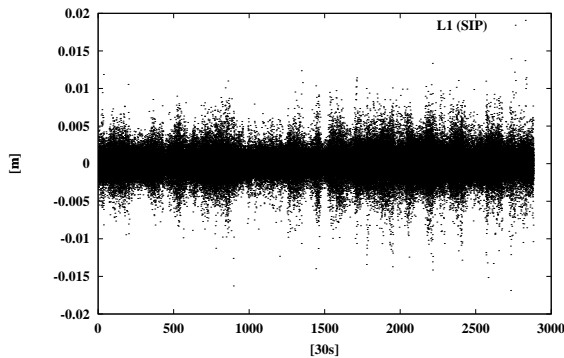


Fig. 3 L_1 -residuals of pseudo clock estimation on day 299 in the year 2000.

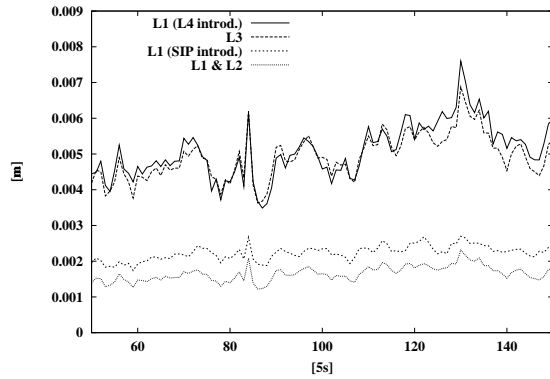


Fig. 4 RMS of pseudo clock estimation in a short interval on day 99 in the year 1999. The chosen approach for realizing a VRR is ' L_1 (SIP introd.)'.

defined observations can only be evaluated on dd level by performing a baseline solution with any independent rover receiver. However for carrier phase observations special attention has to be focussed on the terms I_v^k and $\Delta\rho_{v,trop}^k$ which have to be known precisely for each epoch at the coordinates λ_v, β_v where the VRR should be realized. It is not sufficient in the case of ionospheric delay to adopt values from a standard model as small scale and high frequency fluctuations are not captured. Similar remarks are valid for tropospheric path delay.

3.3.1 Ionosphere Interpolation Model

As for different satellites the different areas in the single layer can be separated by up to 2500 km a satellite specific correction model seems appropriate. Moreover for correcting high frequency variations an epoch-wise modeling is necessary as Traveling Ionospheric Disturbances (TID's) on a medium scale show periods from 10 min up to 1 h. Based on the transformed SIP's δI_i^k on zd level (which reflect the residual part of the ionosphere) a linear correction model at each measurement epoch for each satellite k has to be estimated:

$$\delta I_i^k = \delta I_0^k + \alpha_\lambda \cdot (\lambda_i - \lambda_0) + \alpha_\beta \cdot (\beta_i - \beta_0)$$

with a constant zero difference term δI_0^k , a gradient in east-west direction α_λ , and a gradient in north-south direction α_β . λ_0, β_0 are the coordinates of the Taylor development which do not have to be identical with the coordinates of the VRR. In Figure 5 we compare the interpolated ionosphere parameters (IIP's) for one AGNES site which was not used for interpolation with the original SIP's for the same station.

Both methods show a good agreement in the morning-hours. Towards noon when the ionosphere activity rises the interpolation is less successful but good enough for the VRR (see Section 3.4.2). The quality of the interpolation

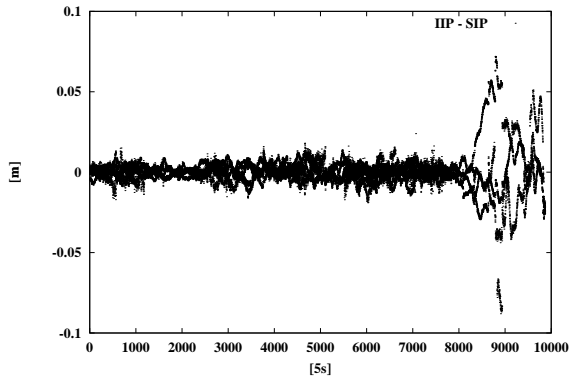


Fig. 5 Difference of IIP's and SIP's for half of the day 99 in the year 1999 for all satellites in Zimmerwald.

mainly depends on the ionospheric conditions and the distance between the stations. The agreement in Figure 5 is based on the central location of the used station Zimmerwald (see Figure 1). A similar experiment at the border of the network would give worse results. Post fit residuals provided by this analysis are typically on a level of 1 cm during night time but may grow up to 20 cm at noon in bad cases. The impact for a VRR will be outlined in Section 3.4.2.

3.3.2 Troposphere Interpolation Model

A similar procedure can be applied to determine the term $\Delta\rho_{v,trop}^k$ for the VRR (see Section 3.3). We model the tropospheric zenith path delay (ZPD) above the VRR using troposphere parameter estimates stemming from a network solution which are available with typical time resolutions of a few hours for the reference sites. This allows us to model the ratio of the observed to the a priori zenith path delay as a linear function of longitude and latitude scaled by an additional height-dependent parameter (Jaeggi, 2001). Experience shows that in AGNES zenith path delays can be modeled at the 1 cm level despite the large variation in height of the stations, the highest receiver being at Jungfrauoch (3635 m above sea level).

3.4 Evaluating Virtual Phase Observations

Artificial phase observations can be processed by any commercial GPS-Software when performing a usual baseline solution. In realistic applications two steps are necessary. First a VRR has to be realized close to the location of the rover receiver. The following step consists of processing the short baseline VRR-rover. To determine the effect of artificial observations on baseline solutions (namely on the ambiguity resolution) we processed data from AGNES for day 099, 1999 in Section 3.4.1 and Section 3.4.2 and data for day 299, 2000 in Section 3.4.2 in different modes.

3.4.1 Baseline Solutions

We computed for five baselines of different length ambiguity fixed solutions between Zimmerwald and another reference station applying a usual wide-lane, narrow-lane ambiguity fixing approach by introducing coordinates and troposphere parameters from previous ambiguity free network solutions. We compare these “real” ambiguity statistics with “virtual” ambiguity statistics obtained from the same baselines where Zimmerwald was replaced by a VRR generated from all the other AGNES sites except of Zimmerwald itself. Table 1 shows the a posteriori RMS of the fractional parts of the wide-lane and the narrow-lane ambiguities.

First we see in both cases a clear linear relationship between the RMS of the wide-lane fractional parts and the baseline length, due to the linear increase of differential ionospheric errors with the baseline length (Beutler *et al.*, 1988), which play the limiting role on wide-lane ambiguity fixing. But more important both quantities tend to be smaller when using virtual observations at one end of the baseline. We recognize that the shorter the baseline the more we gain when using artificial observations. The limiting distance ($\geq 100\text{km}$) where using virtual observations does not show any further improvements heavily depends on the ionospheric conditions.

The narrow-lane fractional parts do not show a similar dependency on the baseline length. But the comparison with real data reveals again a significant improvement.

Next we investigate the effect of different ionosphere modeling on zero baselines as only such baselines are important for realistic applications of VRR where all spatially correlated error terms cancel. Therefore a zero baseline reveals best the quality of the ionosphere modeling. We consider four different modes for establishing a VRR in Zimmerwald and perform a zero baseline solution to the real station Zimmerwald for each mode: (1) original SIP's are applied, (2) IIP's are applied (Zimmerwald used for interpolation), (3) IIP's are applied (Zimmerwald not used), (4) no special ionosphere modeling is applied. The same experiment was carried out with the AGNES site

Table 1. RMS of wide-lane (WL) and narrow-lane (NL) ambiguities for baselines real-real resp. virtual-real of different length

Length (km)	RMS for Real Data		RMS for Virtual Data	
	WL Amb. (WL cycl.)	NL Amb. (NL cycl.)	WL Amb. (WL cycl.)	NL Amb. (NL cycl.)
5.7	0.027	0.035	0.012	0.024
17.0	0.014	0.039	0.012	0.020
79.2	0.036	0.050	0.031	0.034
98.8	0.044	0.034	0.040	0.013
181.6	0.070	0.024	0.074	0.016

Davos which is located at the border of the network. The effects on wide-lane ambiguity fixing are listed in Table 2.

Introducing SIP's gives maximal benefit on ambiguity fixing. Even using IIP's is only slightly worse when including the considered site in the interpolation process. However both modes have no practical use. The mode actually used for generating artificial observations is (3) whose benefit strongly depends on the chosen location in the reference network. For locations near the center the obtained results are of high quality (Zimmerwald in Table 2) while for sites at the border no comparable results can be achieved (Davos in Table 2). No application of any satellite- and epoch specific correction model gives significantly worse results in both cases.

Table 2. RMS of wide-lane (WL) ambiguities for two zero-baselines virtual–real for different procedures of ionosphere modeling (see text)

Procedure	Zimmerwald RMS of WL Amb. (WL cycles)	Davos RMS of WL Amb. (WL cycles)
(1)	0.004	0.011
(2)	0.009	0.012
(3)	0.010	0.035
(4)	0.032	0.059

3.4.2 Realistic Example

Finally we show for one particular day a realistic example from a measurement campaign carried out in October 2000 by the Swiss Federal Office of Topography where code and phase observations were collected by different rover receivers. As in Section 3.4.1 we compute first a VRR in Zimmerwald based on the realistic mode (3) and perform again a zero baseline to the original site. This gives insight into the quality of the expected results. Following the same scheme we compute a VRR for one rover receiver at its location and process the resulting zero baseline. In a first step accurate coordinates are computed using an ambiguity free baseline solution, in a second step ambiguities are fixed to their integer values using a wide-lane/narrow-lane approach. The results are given in Table 3.

The results for the Zimmerwald experiment are even slightly better than those presented in Section 3.4.1 from the year 1999. The results of the rover experiment are slightly worse than all the ones shown previously. In fact, the fractional parts on the rover receiver zero-baseline can not be expected to be as good as for a permanent receiver due to shorter occupation time which demands for different ambiguity resolution strategies.

Table 3. Ambiguity resolution statistics for a zero-baseline from a permanent station resp. rover to a VRR at the same location

Station	WL Amb. (WL cycl.)	NL Amb. (NL cycl.)	Resolved Ambig. %
Zimmerwald	0.006	0.025	100.0 %
Rover	0.012	0.038	93.3 %

4. Summary

We developed artificial code observations which allow to verify the reduced observation noise predicted by theory. The same algorithm is applicable for phase observations when zero difference ambiguity and ionosphere information consistent on double difference level is available. We have shown how this can be done in an efficient way by introducing two assumptions for the transformation of the dd information to the zd level which do not affect the application of artificial observations. Furthermore we have presented four different preprocessing strategies with their advantages and their disadvantages and selected the direct processing of L_1 and L_2 by introducing stochastic ionosphere parameters. This procedure promises not only a high accuracy but allows also for an epoch and satellite specific ionosphere interpolation which can be used to correct rapid ionospheric fluctuations at the location of the VRR.

Our evaluations of artificial observations on baselines virtual–real showed that the width in the distribution of the fractional parts of the ambiguities (wide-lane and narrow-lane) could be reduced significantly helping in fixing them to integer numbers. The ionospheric fluctuations prove to be the limiting factor during daytime.

References

- Beutler, G., I. Bauersima, W. Gurtner, M. Rothacher, T. Schildknecht and A. Geiger (1988). Atmospheric Refraction and other important Biases in GPS Carrier Phase Observations. *Atmospheric Effects on Geodetic Space Measurements*, 12, pp. 15-43.
- Beutler, G., S. Schaer, and M. Rothacher (1999). Wide Area Differential GPS. Internal Report, Printing Office, University of Berne.
- Bock, H., G. Beutler, S. Schaer, T. A. Springer, and M. Rothacher (2000). Processing aspects related to permanent GPS arrays. *Earth Planets Space*, 52, pp. 657-662.
- Jaeggi, A. (2001). Verwendung von Doppeldifferenz-Informationen aus Netzwerklösungen zur Generierung von Beobachtungen einer Virtuellen GPS Referenzstation. Diploma Thesis, Astronomical Institute, University of Berne.
- Mervart, L. (1995). Ambiguity Resolution Techniques in Geodetic and Geodynamic Applications of the Global Positioning System. *Geodätisch-geophysikalische Arbeiten in der Schweiz*, 53, Schweizerische Geodätische Kommission.
- Schaer, S. (1999). Mapping and Predicting the Earth's Ionosphere Using the Global Positioning System. *Geodätisch-geophysikalische Arbeiten in der Schweiz*, 59, Schweizerische Geodätische Kommission.